

# The photochemistry of RDX in solid argon at 10 K

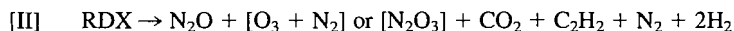
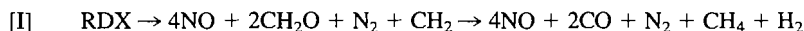
JEFF ALIX AND SUSAN COLLINS

Department of Chemistry, California State University, Northridge, CA 91330, U.S.A.

Received September 4, 1990<sup>1</sup>

JEFF ALIX and SUSAN COLLINS. *Can. J. Chem.* **69**, 1535 (1991).

The photochemistry of RDX was studied in argon matrices at 10 K and examined by FTIR spectroscopy. The spectra and kinetics of product growth indicate that there are two decomposition pathways:

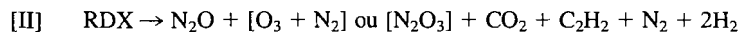
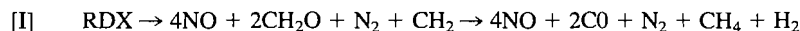


The mechanism II nitrogen products can easily be rationalized for the chair configuration of RDX with axial NO<sub>2</sub> groups adjacent (C<sub>s</sub> symmetry). When considering the carbon products of II, it may be necessary to postulate intermolecular reactions. Our studies gave no evidence for the symmetric triple fission path, which leads to N<sub>2</sub>O and CH<sub>2</sub>O, nor for the NO<sub>2</sub> stripping mechanism reported for the gas-phase thermal reactions, which leads to the formation of NO<sub>2</sub> and HCN. Rather, our findings were more consistent with the known condensed phase products. The production of CH<sub>4</sub>, C<sub>2</sub>H<sub>2</sub>, N<sub>2</sub>O<sub>3</sub>, and O<sub>3</sub> are unique to the matrix study.

**Key words:** RDX, photochemistry, argon matrices.

JEFF ALIX et SUSAN COLLINS. *Can. J. Chem.* **69**, 1535 (1991).

Opérant à 10 K, dans des matrices d'argon et utilisant la spectroscopie FTIR, on a étudié la photochimie du RDX. Les spectres et la cinétique de la croissance des produits indiquent qu'il existe deux voies de décomposition :



La formation des produits azotés par le mécanisme II peut facilement être rationalisée à partir de la configuration chaise du RDX et du NO<sub>2</sub> adjacent axial (symétrie C<sub>s</sub>). Lorsqu'on considère les produits carbonés obtenus par le mécanisme II, il peut être nécessaire de postuler des réactions intramoléculaires. Nos études n'ont pas permis de déceler des données permettant de suggérer l'existence du mécanisme impliquant une voie de fission triple symétrique qui conduirait à du N<sub>2</sub>O et à du CH<sub>2</sub>O ou du mécanisme d'élimination de NO<sub>2</sub> rapporté pour les réaction thermiques en phase gazeuse et qui conduit à la formation de NO<sub>2</sub> et de HCN. Les résultats obtenus sont plutôt en accord avec les produits connus de la phase condensée. La formation de CH<sub>4</sub>, de C<sub>2</sub>H<sub>2</sub>, de N<sub>2</sub>O<sub>2</sub> et de O<sub>3</sub> ne se produit que dans les matrices.

**Mots clés :** RDX, photochimie, matrices d'argon.

[Traduit par la rédaction]

## Introduction

The technique of matrix isolation has proven to be extremely valuable for isolation of intermediates which are crucial in establishing chemical and photochemical mechanisms. 1,3,5-Trinitrohexahydro-*s*-triazine, RDX, is known to decompose by several pathways. The products obtained depend on the phase and temperature of the starting material. The condensed-phase decomposition occurs just above the melting point giving NO, N<sub>2</sub>O, H<sub>2</sub>, CO, CH<sub>2</sub>O, and CO<sub>2</sub> (3). Another study showed that a primary deuterium kinetic isotope effect ( $k_{\text{H}}/k_{\text{D}} = 1.5$ ) is associated with C—H breakage during the rate determining step under these conditions (4). When decomposition is studied at higher temperatures producing gas phase molecules, two other mechanisms predominate (3, 5). The first involves the NO<sub>2</sub> stripping mechanism in which all three NO<sub>2</sub> groups are removed before the triazine fragment decomposes to form HCN and presumably H<sub>2</sub>. The second pathway, which clearly has been seen in molecular beam studies, is the symmetric triple fission to form CH<sub>2</sub>NNO<sub>2</sub> fragments which then further decompose to form CH<sub>2</sub>O and N<sub>2</sub>O (6). Our study was motivated by the possibility of trapping the CH<sub>2</sub>NNO<sub>2</sub> fragment and obtaining its infrared spectrum, and to determine whether the mechanisms in the matrix is similar to the gas or to the condensed phase mechanisms. We report here the matrix FTIR spectra of RDX and its photoproducts and their kinetic behavior at 10 K.

<sup>1</sup>Revision received May 22, 1991.

## Experimental

The apparatus used for these experiments has been described recently (1). FTIR spectra were recorded on a Nicolet 20 DXB instrument with 1.0 cm<sup>-1</sup> resolution. The RDX was deposited by heating it to approximately 200°C in a stainless steel vacuum line positioned in front of the CsI substrate window. Argon was passed over it at 1–2 mmol per h for 1 h. The argon stream entrained the RDX vapors and mixing occurred before deposition. The photolysis light source was an Oriel medium pressure xenon lamp. Broad band irradiation was used for all experiments.

An independent study involving the photolysis of a 1/1/200 matrix of N<sub>2</sub>O/CH<sub>2</sub>O/Ar was necessary to elucidate some mechanistic features. The N<sub>2</sub>O and CH<sub>2</sub>O were deposited by separate jets and combined at the CsI substrate window. A lower limit of approximately five percent reactive pairs is expected at this concentration.

RDX was kindly supplied to us by Dr. Steve Rodgers at the Edwards Air Force Base. Argon (Matheson, 99.995%) and occasionally nitrogen (Airco, 99.995%) were used as matrix gases, and they were used without further purification. No significant experimental differences were found when the reaction was carried out in argon or nitrogen matrices. N<sub>2</sub>O (Aldrich, 95%) was used without further purification. Formaldehyde was prepared from paraformaldehyde according to ref. 2.

## Results

The present section will describe the infrared absorptions of the photochemical products and intermediates in Ar at 10 K.

The infrared spectra of RDX in argon at 10 K are shown in Fig. 1A. Photolysis of RDX is 80% complete in 40 min resulting

TABLE 1. Kinetic behavior of product bands

Frequency ( $\text{cm}^{-1}$ )	Photolysis			Curve in Fig. 2	Kinetics type	Assignment
	2 min	40 min	11 h			
3291.2	0	100	70	—	B	$\text{C}_2\text{H}_2$
2227.5	2	20	100	—	B	$\text{N}_2\text{O}$
2218.9	2	25	100	<i>f</i>	B	$\text{N}_2\text{O}$
2140.0	0	18	100	<i>i</i>	C	CO
2085.0	0	31	100	<i>k</i>	C	CHO
1851.0	0	100	46	<i>c</i>	A	NO
1777.5	0	100	53	<i>d</i>	A	$(\text{NO})_2$
1740.0	20	42	0	<i>a</i>	A	$\text{CH}_2\text{O}$
1693.2	10	50	100	<i>h</i>	B	$\text{N}_2\text{O}_3$
1498.1	20	45	0	<i>b</i>	A	$\text{CH}_2\text{O}$
1300.0	0	23	100	<i>j</i>	C	$\text{CH}_4$
1283.0	2	20	100	—	B	$\text{N}_2\text{O}$
1045.3	4	96	90	<i>e</i>	B	$\text{O}_3$
733.3	4	20	100	—	B	$\text{N}_2\text{O}$
586.3	4	20	100	—	B	$\text{N}_2\text{O}$

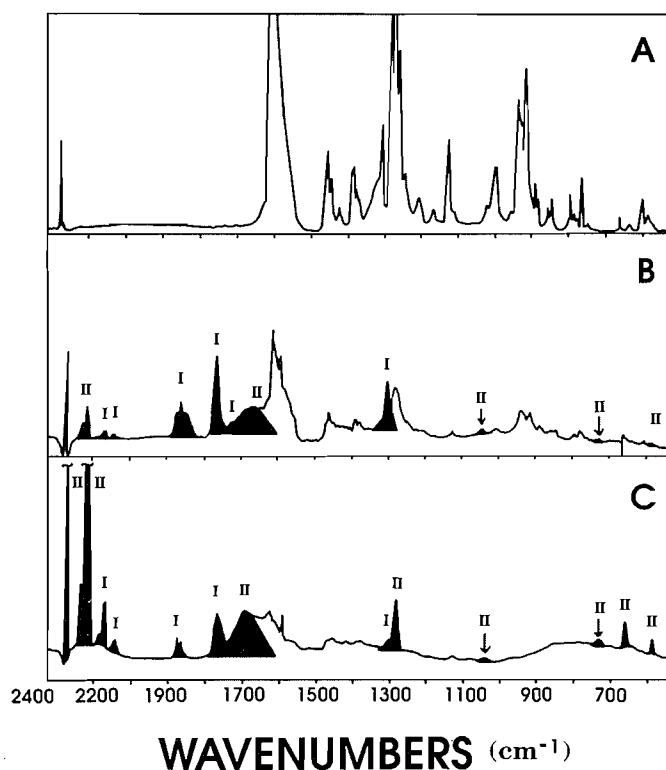


FIG. 1. FTIR absorption bands (A) of RDX in Ar at 10 K, (B) after 40 min photolysis, and (C) after 11 h photolysis. Bands with dark shading are product bands. Bands marked I and II are associated with mechanisms I and II, respectively.

in the product spectrum shown in Fig. 1B. After continued irradiation for 11 h, there is complete disappearance of the RDX bands and evidence of secondary photochemical reactions. Figure 1C shows the photolysis bands after eleven hours. Of the three spectra, only the 40 min spectrum contains RDX and products together as positive bands. The product bands in 1B and 1C are indicated by dark shading. Table 1 gives the frequencies and relative intensities of the product bands, normalized to the most intense band of its kind, at three different

photolysis times. The molecule assignments associated with the listed bands will be discussed in the next section.

Figure 2 illustrates the kinetics of the product bands. Three distinct behavior patterns, types A, B, and C, are illustrated in 2A, 2B, and 2C. Type A behavior is characterized by simple first-order kinetics and by a fast rise at early photolysis times. Type B behavior also is first order, but these bands rise more slowly. At long photolysis times, some bands from types A and B disappear with a concomitant rise of type C bands. Thus at least two examples of consecutive reaction kinetics are seen.

In a separate argon matrix experiment,  $\text{N}_2\text{O}$  and  $\text{CH}_2\text{O}$  were deposited together and photolysed. After 1 h photolysis there was evidence of  $\text{CH}_2\text{O}$  decomposition to form CO, and annealing of the  $\text{N}_2\text{O}$  was evidenced by the sharpening of the  $\text{N}_2\text{O}$  FTIR bands. There was no evidence of any photoreaction between  $\text{N}_2\text{O}$  and  $\text{CH}_2\text{O}$ .

### Discussion

We will discuss the assignment of the product bands and develop a mechanism for the reactions in terms of the kinetic behavior. All of the product molecules are known molecules, and in all cases, literature matrix spectra are available.

#### Mechanism I

**NO.** The bands at 1851.0 and 1777.5  $\text{cm}^{-1}$  are assigned as NO and the  $(\text{NO})_2$  dimer. They follow type A kinetics. These bands appear in a unique portion of the IR spectrum and they compare very well with the literature argon matrix spectra of NO and  $(\text{NO})_2$  (7). After 11 h of photolysis, there appears to be some degradation of both the monomer and dimer.

**CO.** The band at 2140.0  $\text{cm}^{-1}$  follows type C kinetics and is assigned to CO. This band also is very well known and appears in many photochemical studies (e.g., ref. 2).

**$\text{CH}_2\text{O}$ ,  $\text{CH}_4$ ,  $\text{HCO}$ ,  $\text{CH}_2$ .** The bands at 1740.0 and 1498.1  $\text{cm}^{-1}$  appear at early photolysis times with type A kinetics. Consistent with these band frequencies is the molecule formaldehyde (8). The kinetics support the assignment since formaldehyde is known to photolyse in the matrix (9). CO is expected to be a photoproduct, and indeed, the band at 2140.0  $\text{cm}^{-1}$  assigned to CO exhibits type C kinetics. Other

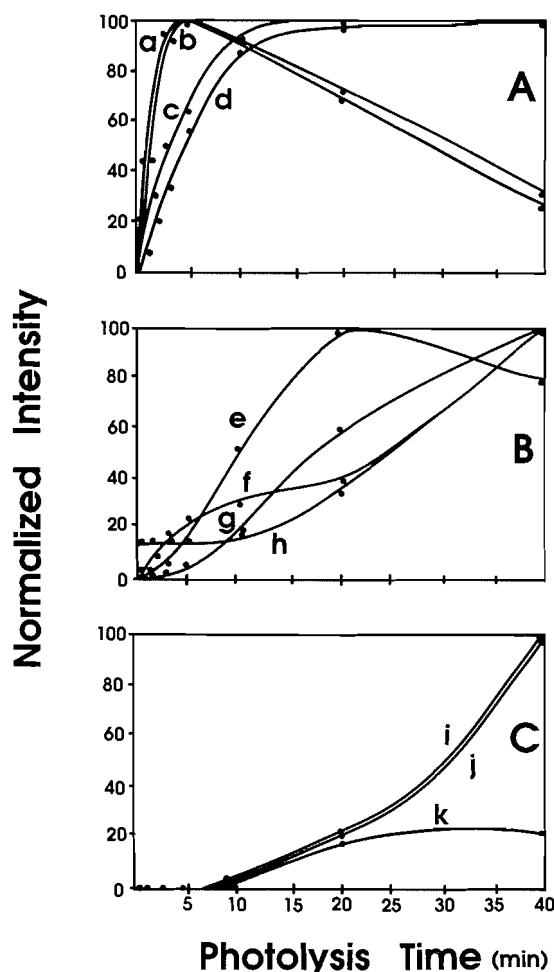
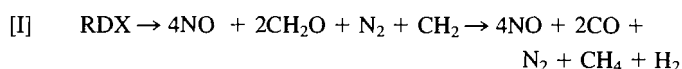


FIG. 2. Normalized FTIR product band intensities versus time. Curves marked a–k are from bands with the following frequencies; a, 1740.0; b, 1498.1; c, 1851.0; d, 1777.5; e, 1045.3; f, 2218.9; g, 733.3; h, 1693.2; i, 2140.0; j, 1300.0; k, 2085.0

bands appearing with type C kinetics due to the decomposition of formaldehyde appear at 1300.0 and 2085.0  $\text{cm}^{-1}$ . We assign these bands as  $\text{CH}_4$  and  $\text{HCO}$  (10, 11). The methane would account for the uptake of hydrogen from the formaldehyde photolysis, conceivably by the reaction of  $\text{CH}_2$  with excited  $\text{CH}_2\text{O}$ . For this, the formation of methylene also must be postulated as a product. To date, there are no literature reports of a matrix spectrum of  $\text{CH}_2$ . All attempts to stabilize methylene under matrix conditions have failed due to its extreme reactivity (12). The band at 2085.0  $\text{cm}^{-1}$  is assigned to formyl. This is tentative at best and at least consistent with the photochemical breakdown of formaldehyde. Another possibility is  $\text{HCN}$ , but this is ruled out since the known band for the  $\text{CH}$  bend at 717  $\text{cm}^{-1}$  is not seen in our experiments. Thus we postulate that one of the decomposition mechanisms of RDX results in  $\text{NO}$ ,  $\text{CH}_2\text{O}$ , and  $\text{CH}_2$  which later react to form  $\text{NO}$ ,  $\text{CO}$ , and  $\text{CH}_4$ . In order to balance the reaction, the production of  $\text{N}_2$  and  $\text{H}_2$  must be postulated to give the overall balanced reaction as:



The  $\text{CH}_4$  band at 1300.0  $\text{cm}^{-1}$  is intense relative to the  $\text{CO}$  band at 2140.0  $\text{cm}^{-1}$  in Fig. 1B, possibly due to some

absorption of the parent RDX overlapping in that region. Alternatively, it may be necessary to postulate extra hydrogen from other sources, i.e., impurities, to react with methylene to give excess methane. Also one should note that a weak absorbance at 1740.0  $\text{cm}^{-1}$  due to formaldehyde still remains in Fig. 1B.

### Mechanism II

$\text{N}_2\text{O}$ . The second decomposition reaction is characterized by type B, slower rise, kinetics. The bands at 2227.5, 2218.9, 1283.0, and 586.3  $\text{cm}^{-1}$  are due to  $\text{N}_2\text{O}$  (13). These bands all follow type B kinetics. As an independent check, an authentic matrix sample of  $\text{N}_2\text{O}$  in argon ( $\text{M/R} = 1/100$ ) was prepared and it gave an identical spectrum.

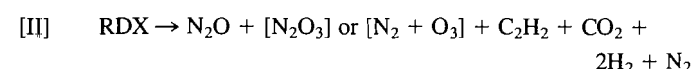
$\text{N}_2\text{O}_3$ . The very broad band at 1693.2  $\text{cm}^{-1}$  has type B growth behavior. This band is assigned as symmetric  $\text{N}_2\text{O}_3$  which has an absorption band at 1690.6  $\text{cm}^{-1}$  in the literature (14). It is known to be a product of the reaction of  $\text{NO} + \text{O}_2$  or  $\text{NO} + \text{O}_3$  in argon matrices. It is not necessary to postulate these reactions, however, since it can form directly from RDX. One could easily envision its formation from RDX in the chair conformation with the axial  $\text{NO}_2$  groups adjacent to each other ( $C_s$  symmetry).

$\text{O}_3$ . A type B band which exhibits consecutive reaction kinetics is at 1045.3  $\text{cm}^{-1}$ . The assignment of  $\text{O}_3$  is consistent with the IR spectrum (15). Such an intermediate certainly would be trapped at 10 K. Further support for this assignment comes from the similarity between the type B kinetics and the known tendency for decomposition under matrix photolysis conditions (16). Again, considering the  $C_s$ -symmetry chair configuration known for solid phase RDX, the two  $\text{NO}_2$  groups are adjacent and they easily could react to form  $\text{N}_2\text{O}$ ,  $\text{O}_3$ , and  $\text{N}_2$  (17).

$\text{C}_2\text{H}_2$ . The next set of type B bands are at 733.3 and 3291.2  $\text{cm}^{-1}$ . These bands also are well known and are easily assigned to acetylene (18). The reaction of two adjacent methylene groups produced from the chair configuration of RDX would give acetylene. The reaction of two methylene groups in the matrix is known to produce highly vibrationally excited ethylene which immediately decomposes to form acetylene and hydrogen (19). As in mechanism I, the presence of another methylene group could conceivably result in the rapid formation of methane.

$\text{CO}_2$ ,  $\text{H}_2\text{O}$ . Comparison of the band at 2340.8  $\text{cm}^{-1}$  in Figs. 1A, 1B, and 1C shows that  $\text{CO}_2$  is present in the deposition spectrum as a consequence of our deposition method. There is only a slight increase during the initial 40 min of irradiation, but there is a dramatic increase during the 11 h photolysis. This is much more than we normally see in this period of time when the background pressure is  $10^{-6}$  Torr. Thus,  $\text{CO}_2$  certainly is a product associated with mechanism II. Matrix water at 1625.0 and 1597.6  $\text{cm}^{-1}$  are seen in our experiments and are very well known to other researchers (e.g., ref. 14). We see normal amounts in the eleven hour spectrum compared to  $\text{CO}_2$  absorbances in the 40 min spectrum, therefore we conclude that water is not a photoproduct of RDX.

If we consider one RDX molecule leading to products, then  $\text{N}_2$  and  $\text{H}_2$  must be postulated to balance the reaction:



This reaction would involve considerable movement of the atoms in forming the carbon products from one RDX molecule.

Alternatively, more than one RDX molecule may participate in the formation of the carbon products.

While mechanisms I and II are consistent with the observed products and kinetic behavior, it might be considered that the two decomposition pathways are not necessarily primary processes, i.e., that the initial fragmentation involves the triple fission or NO<sub>2</sub> stripping mechanisms, and that these intermediates are not stabilized at 10 K. This can be ruled out in any event, since neither NO<sub>2</sub> nor HCN are observed products in our studies. The NO<sub>2</sub> photoproduct NO is seen in mechanism I, but it is not accompanied by HCN. The symmetric triple fission products, N<sub>2</sub>O and CH<sub>2</sub>O, also can be ruled out since our matrix deposition and photolysis of N<sub>2</sub>O and CH<sub>2</sub>O do not give our final mechanisms I or II products. Rather, no reaction occurs between them.

### Conclusions

Reactions [I] and [II] are consistent with the condensed phase thermal chemistry and inconsistent with the gas phase thermal chemistry. The formation of methylene, ethylene, methane, N<sub>2</sub>O<sub>3</sub>, and ozone in our studies seems at first to be different from the known condensed phase chemistry. These differences may be unique to the matrix environment, the cryogenic temperature, the absence of true isolation, and possibly the photochemical process. In the limit that internal conversion is faster than chemical decomposition where thermal and photochemical studies are comparable, the matrix study shows that there must be two pathways leading to the higher temperature condensed phase results. The NO<sub>2</sub> stripping mechanism and the symmetric triple fission mechanism are results of high temperature gas phase studies only.

The conformation of the RDX in the solid phase is known to be the chair configuration with C<sub>s</sub> symmetry. A consequence of the C<sub>s</sub> symmetry is that the NO<sub>2</sub> groups are axial and adjacent. This structure could easily explain mechanisms I and II since no geometric rearrangement of RDX is necessary for product formation except perhaps the carbon products in mechanism II. Furthermore the C<sub>3v</sub> averaged configuration, expected at higher temperatures, has the nitro groups pointing away from each other in the equatorial positions. This structure could more easily explain the stripping NO<sub>2</sub> mechanism and the symmetric triple fission processes seen in the gas-phase studies. Thus

perhaps the barrier to the formation of the C<sub>3v</sub> averaged configuration provides the cutoff, above which the NO<sub>2</sub> stripping and symmetric triple fission mechanisms occur and below which our mechanisms I and II give rise to the condensed phase products. The barrier may be thermal or viscous in nature.

### Acknowledgements

The authors would like to thank Dr. Steve Rodgers from Edward Air Force Base for suggesting this project and supplying us with the RDX. We would like to thank Mary McManamon for the formaldehyde and N<sub>2</sub>O experiments. We also would like to acknowledge partial support from the Universal Energy Systems (grant # 210-S-9MG-115) and partial support from the Petroleum Research Foundation (grant # 19114-GB4) for this project.

1. W. MORAN and S. COLLINS. *J. Mol. Struct.* **222**, 235 (1990).
2. T. MIYAZAWA and K. S. PITZER. *J. Chem. Phys.* **30**, 1076 (1959).
2. M. FARBER and R. SRIVASTAVA. *Chem. Phys. Lett.* **64**, 307 (1979).
4. S. BULUSU, D. WEINSTEIN, J. AUTURA, and R. VELIKY. *J. Phys. Chem.* **90**, 4121 (1986).
5. C. CAPELLOS, S. LEE, S. BULUSU, and L. GAMSS. *Advances in chemical reaction dynamics*. D. Reidel Publishers. 1986. pp. 398-404.
6. X. ZHAO, E. HINTSA, and Y. T. LEE. *J. Chem. Phys.* **88**, 801 (1988).
7. W. GUILLORY and C. HUNTER. *J. Chem. Phys.* **50**, 3516 (1969).
8. H. KHOSHKHOO and E. NIXON. *Spectrochim. Acta*, **29A**, 603 (1973).
9. J. SODEAU and E. LEE. *Chem. Phys. Lett.* **57**, 71 (1978).
10. S. COLLINS, *J. Phys. Chem.* **94**, 5240 (1990).
11. G. EWING, A. THOMPSON, and G. C. PIMENTEL. *J. Chem. Phys.* **32**, 927 (1960).
12. C. B. MOORE, T. D. GOLDFARB, and G. C. PIMENTEL. *J. Chem. Phys.* **43**, 63 (1965).
13. W. B. DEMORE and N. DAVIDSON. *J. Am. Chem. Soc.* **81**, 5869 (1959).
14. S. BHATIA and J. HALL. *J. Phys. Chem.* **84**, 3255 (1980).
15. L. ANDREWS and R. SPIKER JR. *J. Phys. Chem.* **76**, 3208 (1972).
16. D. LUCAS and G. PIMENTEL. *J. Phys. Chem.* **31**, 204 (1939).
17. R. KARPOWICZ and T. BRILL. *J. Phys. Chem.* **88**, 348 (1984).
18. A. ENGDAHL and B. NELANDER. *Chem. Phys. Lett.* **100**, 129 (1983).
19. Y. P. LEE and G. C. PIMENTEL. *J. Chem. Phys.* **75**, 4241 (1981).